Received: 8 September 2023 | Revised: 26 February 2024 | Accepted: 27 February 2024

DOI: 10.1002/nano.202300134

RESEARCH ARTICLE

Nano Select Open Access WILEY

Antibacterial performance of a copper nanoparticle thin film

Intisar Salah[1] | **Elaine Allan**[2] | **Sean P. Nair**[2] | **Ivan P. Parkin**[1]

[1]Materials Science, Department of Chemistry, University College London, London, UK

[2]Department of Microbial Diseases, UCL Eastman Dental Institute, Royal Free Campus, London, UK

Correspondence
Intisar Salah, Materials Science, Department of Chemistry, University College London, 20 Gorden Street, London, WC1H 0AJ, UK.
Email: intisar.salah.19@ucl.ac.uk

Funding information
EPSRC Centre for Doctoral Training in Molecular Modelling and Material Science, Grant/Award Number: EP/L015862/1

Abstract

The prevalence of the SARS-CoV-2 virus has led to an increased focus on cleaning and disinfecting surfaces in the community and hospitals. An inherently antibacterial thin film is reported to combat the transmission of microbes on glass surfaces that could be accessed by the public, reducing the need for constant cleaning. The copper nanoparticle thin film is synthesized via a sol–gel method and deposited using a dip-coater to create a transparent, rugged film resistant to scratching. The antibacterial performance is tested by a droplet and an aerosol deposition technique, where *Escherichia coli* and *Staphylococcus aureus* are sprayed directly onto the thin film, replicating coughs and sneezes: a common form of microbial transmission. The mechanism of antibacterial performance is studied by introducing reactive oxygen species quenchers to the thin film. This research presents copper nanoparticle thin films as an effective solution in reducing the transmission of microbes on glass surfaces and their potential as a valuable tool in preventing the spread of infectious diseases.

KEYWORDS
antimicrobial, copper nanoparticles, reactive oxygen species, sol–gels, thin films

1 | INTRODUCTION

The COVID-19 pandemic has given rise to a more hygiene-conscious society. As a result, there is a new appreciation of the potential for antimicrobial coatings on surfaces used by the public in the community and hospitals. Pathogenic bacteria, viruses, and fungi are commonly transmitted via four modes: direct physical contact, indirect contact of a surface, droplets or aerosols in the environment.[1] They can lead to healthcare-acquired infections (HAIs) and community-acquired infections (CAIs).[2–4] By preventing the adhesion of microbes to surfaces, a major transmission route is targeted, as almost 50% of HAIs are caused by contact with contaminated surfaces.[5–7] Droplets and aerosols account for 15%; these are considered a direct form of transmission since they require an infected person to cough or sneeze and the recipient to inhale the aerosols and droplets.[8,9] Aerosols can easily be inhaled as they are less than 5 μm in diameter.[10] Aerosolization of the infection can lead to particles remaining in the air for hours as smaller particles have a longer half-life.[11,12]

As aerosols are released in coughs and sneezes, placing a volume of bacterial suspension on top of antibacterial surfaces is not close to the real-world transmission of microbial infections. Instead, spraying the suspension to create aerosols is an alternative method to test the performance of antibacterial samples. In this work, we have used a spraying technique and the microbiological

method described in ISO-22196 to test thin films designed for application to glass surfaces intended for use in public spaces.

With stylish glass surfaces becoming more common in public spaces, the inherent ability of microbes to adhere to such surfaces needs to be considered. Choosing an appropriate antimicrobial agent for inclusion in a thin film depends on the surface's intended application. For instance, an essential criterion for a glass surface to be used as a touchscreen device is that the glass is completely transparent. A way to achieve this is to develop a film with nanoparticles. Transition metals such as copper, gold, and silver are key agents that can functionalize thin films to achieve antimicrobial activity.[13] Copper is a readily available and relatively inexpensive element. Improvements in nanotechnology in recent years have led to a focus on developing copper nanoparticle (CuNP) thin films. They have a larger surface-area-to-volume ratio resulting in increased toxicity compared to the untreated metal, as well as improved optical properties making them desirable for coating glass.[14,15]

Methods employed to make CuNP thin films include sol–gel technique, chemical vapor deposition, evaporation techniques, and sputtering.[16] The method utilized in this research was the sol–gel technique, where an alkoxysilane precursor solution was formed and CuNPs were added to the matrix after. Then, the sol–gel was coated on a glass substrate via dip-coating, where the glass was dipped into the sol–gel and removed at a controlled pace to ensure the solvents had time to evaporate, leaving the desired nanoparticles on the surface. This method is recognized for its ability to produce homogeneous nanoscale structures that exhibit physical rigidity and optical transparency.[17,18]

In the microbiology experiment, reactive oxygen species (ROS) quenchers were introduced to the bacterial suspension to investigate the bactericidal mechanism of the thin film. These quenchers selectively scavenge the ROS produced by the antimicrobial thin film, helping to elucidate its specific impact on bacterial viability. ROS are endogenous species that are essential in cellular metabolism and in the immune systems of eukaryotes.[19] However, if ROS are formed in excess, the cell is overwhelmed. This can be toxic to the cell resulting in membrane damage and an oxidative stress response, causing cell death.[20–22] Therefore, a possible way of inducing a bactericidal response by a thin film is by intentionally generating excess ROS. In this case, the introduction of CuNPs was theorized to induce such a response. If the CuNP film's exposure to the bacteria leads to ROS generation, a reduction in the recovered bacterial count is visible without the quencher. Then, with the presence of a ROS quencher, a higher number of bacteria would be recovered as the quencher would inhibit ROS formation. Thus, by introducing ROS quenchers to the bacterial suspension, an understanding of the ROS responsible for the antibacterial activity of the thin film can be made by comparing the activity with and without the quenchers.

In the present work, a transparent layer of copper and silica nanoparticles was deposited to form a thin film on a glass substrate. The precursor solution was formed using the sol–gel method and deposited by dip-coating. After analysis was performed to understand the surface properties, the films were incubated with *E. coli*, a Gram-negative bacterium, and *S. aureus*, a Gram-positive bacterium, to establish the film's antimicrobial abilities. The film's antibacterial properties were explored using a droplet method and an aerosolized inoculum alongside a mechanistic study to determine the responsible ROS for the thin film's antibacterial activity.

2 | EXPERIMENTAL AND CHARACTERIZATION

2.1 | Thin film synthesis

2.1.1 | Materials

Tetraethyl orthosilicate (TEOS, 98%), diacetone alcohol (99%), citric acid (99.5%), isopropanol (98%), and acetone (99.5%) were purchased from Sigma Aldrich UK. Copper nanopowder was produced by NANOTEC. The clear float glass (dimensions: 1 cm × 1 cm × 0.4 cm) was supplied by Pilkington NSG Ltd. Copper foil (99.95%) was purchased from Merck.

2.1.2 | Method

In this study, a transparent antibacterial thin film was developed for glass using a sol–gel method and a dip-coater to deposit the film. First, to synthesize a 2.5 wt% silica sol–gel, TEOS was hydrolyzed by reacting TEOS and diacetone alcohol in a ratio of 1:2.75 mol then adding citric acid (0.27 g, 100 mmol) as a catalyst. The precursor solution was left to stir for 4 hours to form hydrolyzed species to later form silica nanoparticles. Next, it was left in a fridge overnight to aid in condensation and hence, the formation of the siloxane bonds (Si–O–Si). This method yielded silica nanoparticles, forming the matrix for the CuNPs. Copper nanopowder prepared via electrolysis was then added to polymerized TEOS in a ratio of 1:0.006 mol of isopropanol to CuNPs (6.3 mmol). The glass was cleaned with deionized water, acetone, and isopropanol, before being left to dry. The cleaned glass squares (1 cm × 1 cm × 0.4 cm) were dip-coated into the sol–gel and removed at a rate of 600 mm min^{-1}, five times. Each layer was allowed to dry completely to ensure all solvents had evaporated. The coated samples were then thermally

annealed at 200°C for 40 minutes, resulting in a film thickness of approximately 330 nm.

2.2 | Thin film analysis

X-ray photoelectron spectroscopy analysis was performed to determine the elemental composition and chemical states of the film's surface as the instrument is sensitive to the particles on the surface (approximately 10 nm).[23,24] Thermo Scientific X-ray photoelectron spectrometer with a monochromatic Al Kα X-ray source (1486.96 eV) and depth profiling using an argon gun was performed at 0 nm (sample surface) and 60 nm (inside the sample). The data were calibrated against the C 1s peak (284.5 eV) and fitted using CASA XPS software.

A Jeol 7600F Scanning Electron Microscope (SEM) was employed to determine the surface topography. First, the samples were coated with gold crystals for 10 seconds through an argon sputter coating process, and then the topography was observed by SEM at an accelerating voltage of 5–15 kV.

Transmittance spectra were recorded in the wavelength range between 200 and 800 nm, employing a Shimadzu UV-3600i Plus UV–vis spectrophotometer. Blank glass was used as a reference.

Static water contact angle measurements were performed with a KRUSS DSA25E Drop Shape Analyzer at ambient temperature with a 7 μL deionized water droplet as the indicator. All the contact angles were determined by averaging values measured at three different points on each sample surface.

The thin film's resistance to scratching was measured using an Elcometer 501 Pencil Hardness tester with various hardness values of graphite pencils ranging from 6B to 6H, with 6H being the hardest. After sharpening and flattening the tips with sandpaper, the pencils were mounted in a weighted apparatus with wheels applying a force of 7.5 N. The tips were lowered onto the sample surface at an angle of 45°, and the weight was manually moved across the film. This process was repeated to assess hardness consistency. The pencil hardness was systematically increased until the surface was scratched, and the durability was measured as the maximum hardness of the surface that could endure the force without scratching.

2.3 | Bacterial culture

2.3.1 | Media and chemicals

The MacConkey (MAC) agar, Mannitol salt agar (MS) agar, Brain-heart-infusion (BHI) agar and phosphate-buffered saline (PBS) were purchased from Oxoid Ltd., UK. All other reagents were purchased from Sigma Aldrich UK. ROS quenchers were made up in PBS except mannitol which was solubilized in deionized water. The microscope slides were purchased from VWR.

2.3.2 | Bacterial strain

Antibacterial activity was tested against *Escherichia coli* ATCC 25922 and *Staphylococcus aureus* 8325-4. Ten millilitres of BHI broth was inoculated with one bacterial colony and cultured in a shaking incubator in air (37°C, 200 rpm, 18 h). UV–vis spectrophotometry was used to measure the turbidity of the overnight broth at 600 nm to confirm that the culture reached 10^9 CFU mL^{-1}. The bacteria were recovered by centrifugation (21°C, 4000 rpm, 5 minutes) and washed in PBS (10 mL). This was repeated twice, and then the bacterial pellet was re-suspended in 10 mL of PBS and diluted 1000-fold to obtain an inoculum of ~10^6 CFU mL^{-1}. This inoculum served as a negative control, and blank glass, subjected to the same bacterial exposure as the CuNP samples, was also employed as a negative control as the control glass. As blank glass lacks antimicrobial activity, theoretically, the values for the control inoculum and the control glass should be identical. The copper foil was subjected to the same bacterial exposure as the CuNP samples and was used as a positive control.

2.3.3 | Exposing the thin film to *E. coli* and *S. aureus*

To expose the thin film to a droplet of bacteria, 50 μL of the bacterial suspension at ~10^6 CFU mL^{-1} was added to the thin film and left to incubate for 1.5 hours in either a dry chamber or a humidity chamber. To create a dry sample chamber, the samples were placed on a petri dish, a droplet was added on top of the film, and the lid was placed on top. For the humid chamber, filter paper was put in a 90 mm petri dish and wetted with 2 mL PBS, then the lid was placed to maintain the humidity. An untreated inoculum of ~10^6 CFU mL^{-1} served as a negative control alongside control glass that was exposed to the bacteria via the droplet method, while copper foil (99.95%) that was also exposed to the bacteria via the droplet method was used as a positive control. Copper foil has been proven to be an antibacterial metal that kills 99% of bacteria therefore its performance is compared to its nanoparticles in this research as a positive control.[25–27] The controls are described in Table 1.

For the aerosol deposition, the bacterial suspension was sprayed onto the thin film with a Timbertech Airbrush Kit. The sample holder was sterilized with 70% ethanol, cleaned with deionized water, and then allowed to dry.

TABLE 1 Names and descriptions of the samples and controls used in this research.

Name	Sample or control	Description
CuNP thin film	Sample	The CuNP thin film synthesized in this study using the sol–gel method and deposited using a dip-coater
Control inoculum	Negative control	The untreated inoculum of ~10^6 CFU mL^{-1} of either *E. coli* or *S. aureus*
Control glass	Negative control	The untreated cleaned float glass which is the same glass as the CuNP thin film substrate
Cu foil	Positive control	Pure copper foil (99.95%)

A dilution of 10^6 CFU mL^{-1} *E. coli* and *S. aureus* in PBS was tested in triplicate. First, 5 mL of the bacterial suspension was transferred onto the sterilized sample holder. Then, the 1 cm^2 thin films, control glass, and copper foils were placed in a 6-well plate, with one sample in each well, and positioned at a 45° angle at the back of a microbiological safety cabinet (Contained Air Solutions (CAS) BioMat 1 class 1 microbiological safety cabinet, compliant with EN 12469:2000). The suspension was sprayed 20 cm away from the samples for 5 seconds using compressed air and left to dry for 30 minutes in a dry chamber. A control inoculum of ~10^6 CFU mL^{-1} served as a negative control alongside the control glass that was exposed to the sprayed bacteria, while copper foil (99.95%) that was also exposed to the sprayed bacteria was used as a positive control.

2.3.4 | Determination of antibacterial activity by viable counting

To determine the antibacterial activity of samples, viable counts were performed according to ISO-22196. After incubation, the samples were added to 900 µL PBS and vortexed. Next, 600 µL was removed and added to an Eppendorf tube that was placed in the sample holder of the Interscience Diluter and Plater. Each sample was diluted to 10^6 and plated on MacConkey agar (*E. coli*) or mannitol salt agar (*S. aureus*). The plates were incubated aerobically at 37°C at 95% relative humidity and counted on an Interscience Scan Colony Counter after 24 hours (*E. coli*) or 48 hours (*S. aureus*).

2.3.5 | Quencher studies

To understand the impact of reactive oxygen species on the thin film performance, quenchers were employed by adding them to the bacterial suspensions before application to the materials as described above. 2 mM of L-histidine ($^1O_2$), 10 units mL^{-1} of catalase (H_2O_2), and 20 units mL^{-1} of superoxide dismutase ($^\circ O_2$) were dissolved in PBS and 82 mM of mannitol ($^\bullet OH$) was dissolved in water. These solutions were filtered through a 0.22 µm membrane and added to the overnight culture of *E. coli* and *S. aureus*. The tests were conducted in humid conditions, the same way as the viable counts described above. A control inoculum of ~10^6 CFU mL^{-1} served as a negative control alongside a control glass that was exposed to the sprayed bacteria, while copper foil was used as a positive control.

2.3.6 | Statistics

A one-tailed Mann–Whitney *U* test of the results was calculated to obtain statistical data using SPSS Statistics software (IBM SPSS Statistics for Macintosh, Version 29.0, Armonk, NY, USA). If $p \leq 0.05$, the value is considered significant and if $p > 0.05$, insignificant.

3 | RESULTS AND DISCUSSION

3.1 | Characterization

3.1.1 | XPS

X-ray photoelectron spectroscopy (XPS) was deployed to detect the chemical states of elements present up to a depth of 10 nm on the surface of the thin film.[23,24] From the XPS survey spectra in Figure 1A, the presence of copper (952.5 and 932.5 eV) can be determined, as well as Si (102.8 eV), O (531.3 eV), and C (284.6 eV). To further analyze the film, high-resolution spectra of Cu 2p, Si 2p, O 1s, and C 1s were obtained, as shown in Figure 1B–E. The Cu 2p region in Figure 1B showed that copper atoms were present as Cu(0).[28,29] The Si 2p peak in Figure 1C was deconvoluted into two peaks: Si-O_2 (102.9 eV) and organic Si (102.6 eV). The O 1s peak at 531.3 eV in Figure 1D was deconvoluted into three peaks: O–Si (531.2 eV), O C (529.9 eV), and O C (532.6 eV). The peak observed at 284.6 eV corresponds to carbon and was deconvoluted into three peaks: C C/C H (283.6 eV), C O (283.7 eV), and C O (287.5 eV). The Si 2p and O 1s signals act as markers for determining the presence of silica nanoparticles; the peaks in the Si 2p and O 1s spectra (Figure 1C,D) at 102.8 and 532.2 eV confirm the presence of silica nanoparticles.[30]

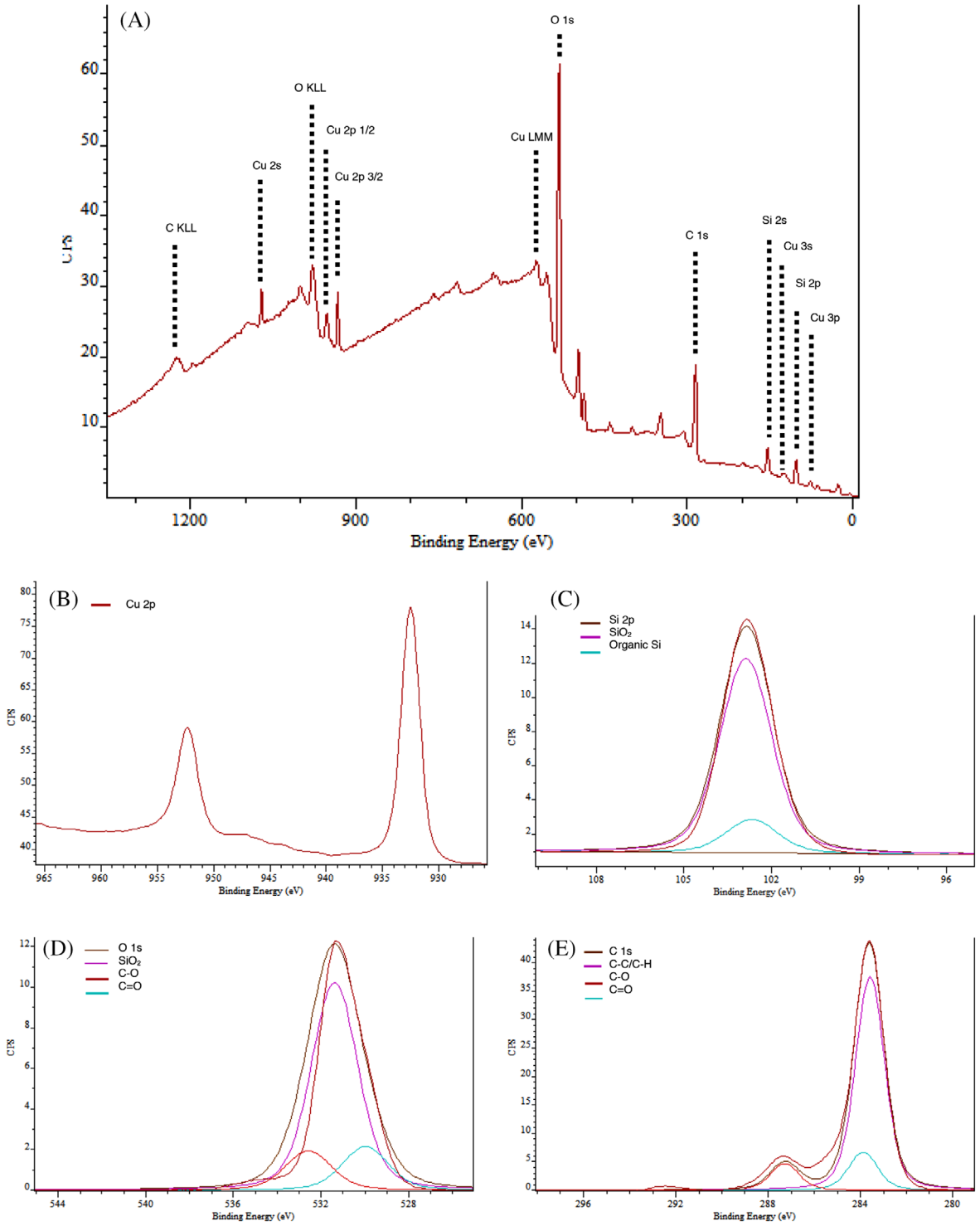

FIGURE 1 XPS survey of the CuNP thin film (A) and the high-resolution spectra of Cu 2p (B), Si 2p (C), O 1s (D), and C 1s (E). The binding energy is measured in eV.

3.1.2 | SEM

The SEM images were obtained to determine the thin film's nanoparticle sizes, distribution, and homogeneity. In Figure 2, the thin film demonstrates a broad particle size distribution range due to the electrolytic deposition method by which they were manufactured. This method produces non-planar surfaces and uniformity is difficult to maintain. However, it is a low-cost, simple, and easily tuneable method compared to more complicated mechan-

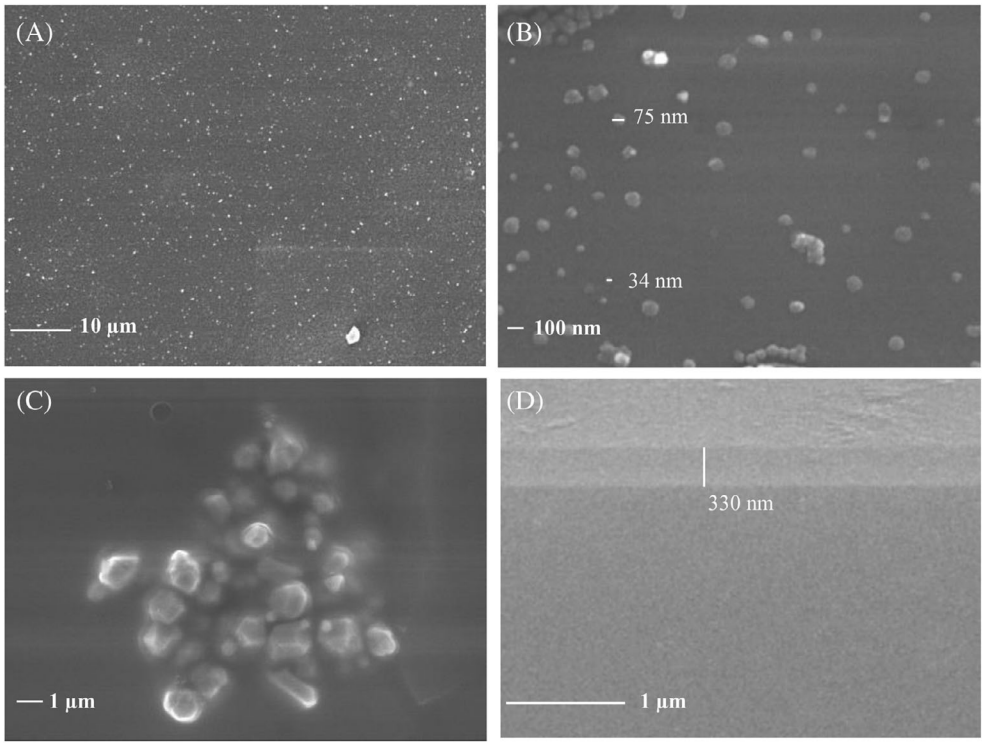

FIGURE 2 SEM images of the CuNPs thin film demonstrating the even distribution of CuNPs (A), a high magnification image of the CuNPs (B), a high magnification image of a CuNP aggregate (C), and an angled cross-sectional image demonstrating the film thickness (D). From images (B) and (C), the nanoparticle size can be estimated to be ranging from 30 nm to 1 µm. Image (D) demonstrates the film thickness at ~330 nm with the substrate beneath it and the film surface above.

ical milling and chemical reduction. As anticipated, the nanoparticles are well distributed and the scattering of the CuNPs is evident.

3.1.3 | UV-visible spectrometry

A UV-visible spectrometer was used to test the optical transparency of the thin film. The transmittance was examined in the wavelengths 200–800 nm. Figure 3 shows the UV–vis spectra of the CuNP film and is compared with the UV–vis spectra of the control glass. The control glass achieved a 90% light transmittance in the visible range. Considering the control glass is 0.4 cm thick, a lower than 100% transmission was anticipated as the thicker glass increases the probability of absorption as the light traverses a longer path through the material and the greater substrate volume for light to interact with causes scattering.[31,32] From the spectra, it was observed that the transparency was reduced by 20% in the CuNP thin film. As the thin film is only 330 nm thick, it maintains transparency throughout the entire visible light range while the absorbance peak occurs at approximately 365 nm, with a sharp decline in transmittance to zero. The film also exhibits good optical transparency in visible light by the human eye as demonstrated by the photograph in Figure 4.

3.1.4 | Water contact angles

Studies to understand the surface properties were initiated with measurements of the water contact angles of the thin film. These data give an insight into how microorganisms interact with the thin film and their adhesion to the surface. Increasing the hydrophobicity of the surface creates an unfavorable environment for microbes as it's more challenging for them to adhere.[33–35] For a surface to be considered hydrophobic, it needs to have a contact angle greater than 90° and for it to be superhydrophobic, more than 150°.[36] A superhydrophobic surface reduces friction between the water droplet and the film; therefore, such a surface is unfavorable for microbial adhesion.[37–39] This is the main principle behind self-cleaning surfaces and is an important property for the glass coatings used outdoors, in public spaces and in high-footfall locations.[40,41] The contact angle results in Figure 5 suggest that the thin film has similar hydrophobic properties to the copper foil with a 92.1° angle for the thin film and 99.6° for the copper foil. The high WCA impacts the surface activity with bacterial

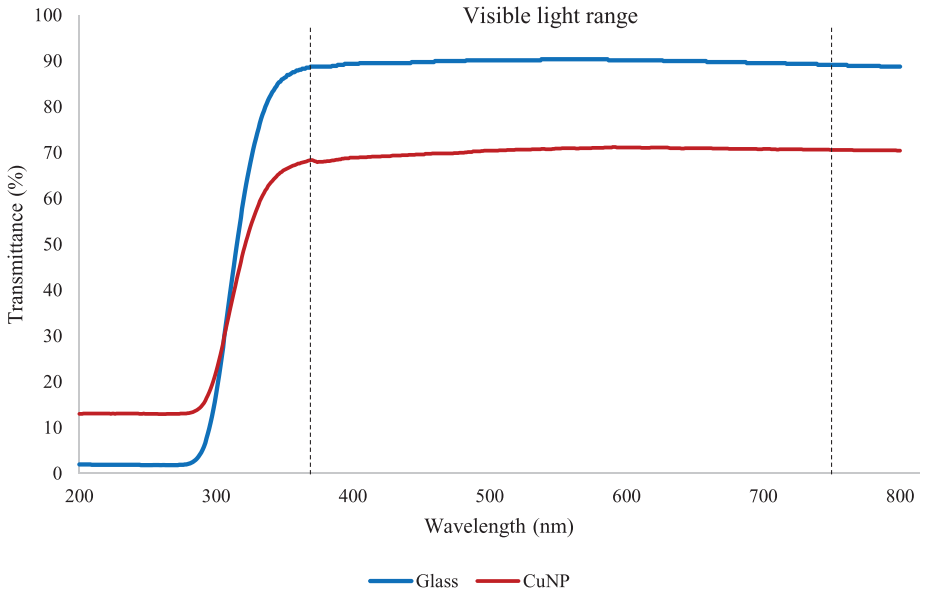

FIGURE 3 UV-Visible spectra comparing the transmittance of control glass (blue) and the CuNP thin film (red). The visible light range is indicated by the dotted lines between 380 and 750 nm.

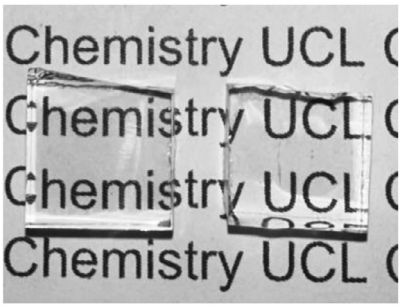

FIGURE 4 Photograph of the control glass (left) and the CuNP thin film (right) demonstrating the high level of transparency of the thin film.

suspensions, thus suggesting the thin film may possess antimicrobial activity.[42–44]

3.1.5 | Scratch resistance

The thin film's ability to resist scratching was tested using an Elcometer equipped with pencils of varying hardness values of graphite. The film was scratched with the pencils ranging from the softest, 6B, to the hardest, 6H. A 6H hardness was attainable as the CuNP thin film was able to withstand all the scratches suggesting a hard and scratch-resistant film.

3.2 | Antibacterial activity

The antibacterial activity of the CuNP thin film was tested against *E. coli* ATCC 25922 and *S. aureus* 8325-4. The bacterial colonies were diluted to obtain an inoculum of approximately 10^6 CFU mL^{-1}, which was also used as a negative control. The thin film was exposed to *E. coli* and *S. aureus* using two methods: a droplet method using ISO-22196 and an aerosol deposition method. Additionally, the impact of reactive oxygen species on the thin film's performance was studied by adding quenchers L-histidine, mannitol, catalase, and superoxide dismutase to the bacterial suspensions before incubating with the films. The droplet tests were conducted in humid and dry conditions, while the quencher studies were conducted in humid conditions only. Copper foil was used as a positive control, and control glass was used as a second negative control.

To calculate the performance of the CuNP thin film, Equation (1) below, was used.

$$\text{Antibacterial activity (\%)} = \frac{(C - S)}{C} \times 100 \qquad (1)$$

C refers to the number of colonies (CFU mL^{-1}) recovered from the control glass after exposure to the bacteria and *S* is the number of colonies (CFU mL^{-1}) recovered from the thin film after exposure to the bacteria.

3.2.1 | Viable count of droplet inoculum

In accordance with the ISO-22196 protocol, the antibacterial performance was tested in humid conditions. However, tests in dry conditions were also conducted since dry conditions closely mimic real-life circumstances, where microbes naturally desiccate and die.[45,46] This is due to the high stress they experience without water,

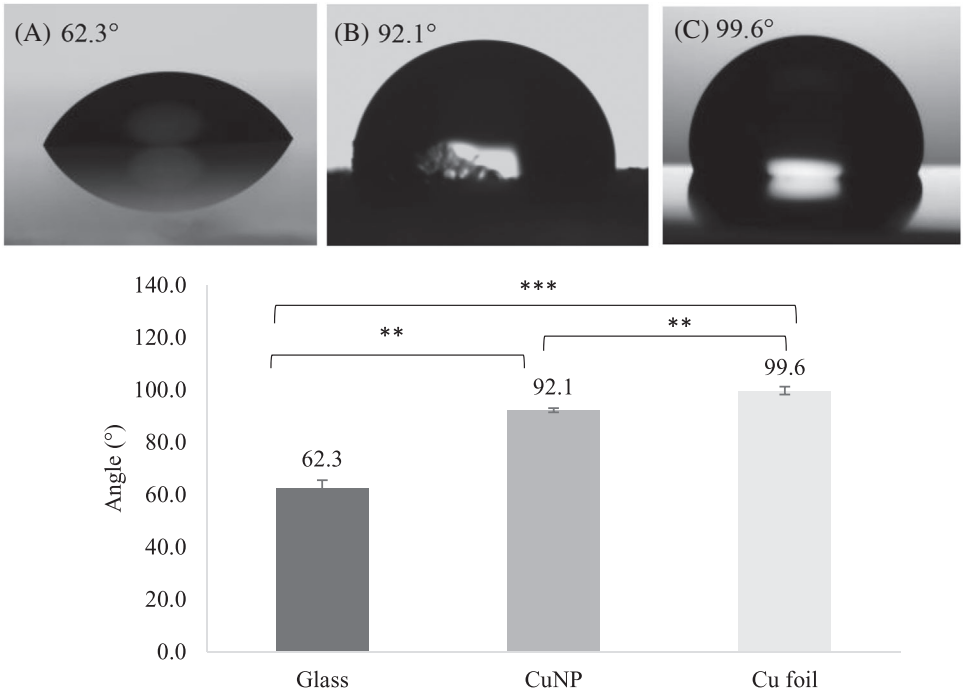

FIGURE 5 The static water contact angles of control glass (A), dip-coated copper nanoparticle (CuNP) thin film (B), and copper foil (C). (D) This is a graphical demonstration of the results alongside the statistical analysis of significant differences where ** means $p \leq 0.01$ and *** means $p \leq 0.001$. The thin film has a contact angle similar to the copper foil though neither is considered superhydrophobic. Nonetheless, the hydrophobic nature of the film ensures it is not a favorable surface for microbes to settle.

leading to numerous physiological consequences resulting in bacterial death.[45,47] Therefore, even without exposure to an antimicrobial surface, increased cell death is expected in dry conditions with fewer bacteria recovered than in humid conditions, where microbes thrive.

Figure 6 shows the bactericidal activity of the thin film coating against *E. coli* and *S. aureus* after a 1.5 h incubation time in humid and dry conditions. In Figure 6A, no reduction in the number of viable bacteria was observed on the control glass in comparison to the control, the *E. coli* inoculum that was not exposed to glass ($p > 0.05$, Mann–Whitney *U* test). However, a statistically significant reduction was observed in *E. coli* with a 99.4% reduction in colonies in humid conditions ($p \leq 0.05$, Mann–Whitney *U* test) and a 99.7% reduction in dry conditions after exposure to the thin film compared to control glass ($p \leq 0.01$, Mann–Whitney *U* test). Following exposure to the copper foil, the bacterial count was below the limit of detection ($<10^2$ CFU mL^{-1}), indicating more than a 99.98% reduction in viable bacteria. This was expected as copper has intrinsic antimicrobial properties.[48–51] In Figure 6B, no reduction in the number of viable bacteria was observed on the control glass in comparison to the control, the original *S. aureus* inoculum ($p > 0.05$, Mann–Whitney *U* test). However, a statistically significant reduction in the number of *S. aureus* colonies was observed with a 99.2% reduction in cells incubated in humid conditions and a 99.8% reduction in dry conditions when exposed to the thin film, compared to the control glass ($p \leq 0.001$, Mann–Whitney *U* test).

The *E. coli* and *S. aureus* exhibited increased susceptibility to the thin film in comparison to the control glass; both bacteria demonstrated a statistically insignificant difference in the results of the humid and dry conditions ($p > 0.05$, Mann–Whitney *U* test). A lower recovery of colonies is anticipated when testing in an environment lacking humidity since bacteria desiccate in dry conditions.[45–47] However, statistically, these results don't showcase this tendency, suggesting that the number of bacteria dying from drying out in the 1.5 hours incubation period is lower than anticipated and thus doesn't impact the results.

3.2.2 | Viable count of aerosolized inoculum

Studies have demonstrated that coughs expel approximately 3000 droplets and 40,000 from sneezes.[52,53] The aerosol deposition tests aimed to elucidate the effectiveness of the thin film using a sprayed inoculum to imitate the real-world scenario of coughs and sneezes. To replicate this, a dilution of 10^6 CFU mL^{-1} bacteria was used, equivalent to that used in the standard droplet technique.

In Figure 7, a statistically significant difference was observed between the control glass and the thin film for both *E. coli* and *S. aureus* ($p \leq 0.05$, Mann–Whitney *U*

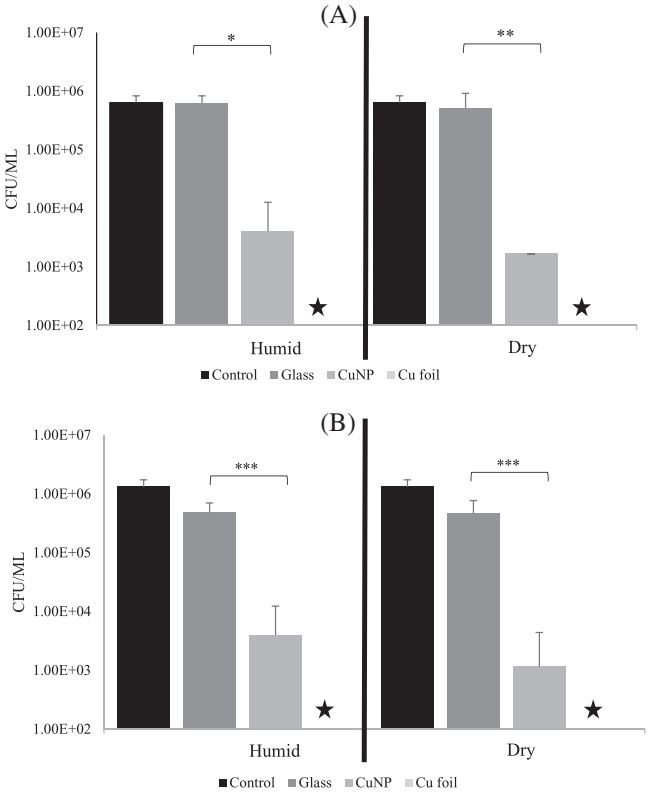

FIGURE 6 Bactericidal activity of the thin film samples against a droplet of *E. coli* (A) and *S. aureus* (B) after 1.5 hours of exposure in humid and dry conditions and at a constant temperature of 20°C. The control was the control inoculum that had not been treated. The glass was control glass included as the negative control and copper foil as the positive control. Star () indicates the copper foil for which the count was below the detection limit of 10^2 CFU mL^{-1}. * means $p \leq 0.05$, ** means $p \leq 0.01$, and *** means $p \leq 0.001$. Data presented as mean ± SD.

test). From Figure 7A, a 94.7% reduction in the number of *E. coli* colonies recovered was observed. For the *S. aureus* in Figure 7B, a 97.2% inactivation of viable colonies was observed ($p \leq 0.001$, Mann–Whitney *U* test). This suggests that the bactericidal performance of the CuNP thin film is reduced when the inoculum is sprayed in comparison to the droplet tests in Figure 6. Given the inherent loss of bacterial suspension to the environment when sprayed, a lower bacterial recovery from the control glass and the thin film was anticipated when sprayed in comparison to the droplet tests. This could be due to the aerosolized bacterial suspension dispersing more widely, leading to a lower concentration of bacteria per thin film sample. This dilution effect could reduce the efficacy of the antimicrobial agents in the film.

Considering the initial 10^6 CFU mL^{-1} dilution in the aerosol test is the same concentration used in the droplet tests, it is anticipated that the number of cells recovered should be similar. However, in Figure 7, there is a 10-fold decrease in bacteria recovered from the control glass in comparison to the number of bacteria recovered from the control glass in droplet tests in humid conditions in Figure 6. This 10-fold decrease was observed in both *E. coli* and *S. aureus*. Although a larger surface area of the film is exposed to the bacterial suspension in the aerosol tests, a potential explanation for the decrease in recovered bacteria could be that when the suspension is sprayed, it spreads thinly over the surface. This thin spreading makes the bacteria more susceptible to drying out and a lower number of bacteria is therefore recovered.[45,46]

3.2.3 | Detection of reactive oxygen species

It is essential to understand the mechanism of bactericidal activity to ensure the best antibacterial performance of a thin film. One proposed mechanism of CuNP-induced microbial death is the induction of reactive oxygen species (ROS) through Fenton-like and Haber–Weiss reactions.[54,55] These are singlet oxygen ($^1O_2$), hydroxyl radicals (•OH), hydrogen peroxide (H_2O_2), and superoxide radicals ($^\circ O_2$) that are derived from molecular oxygen and can be quenched through endogenous systems. In this scenario, the number of ROS formed outweighs the cell's capacity to remove them, leading to oxidative stress that can cause irreversible damage to the bacteria resulting in cell death.[56] Thus, tests were conducted with ROS quenchers to see if their presence inhibits the activity of the CuNP thin films.

The ROS quenchers were added to separate bacterial suspensions. Fifty microliter of each bacterial suspension was placed on a separate thin film and left to incubate for 1.5 h in humid conditions. The impact of the ROS quenchers on the CuNP film against *E. coli* can be observed in Figure 8A. The $^1O_2$ and $^\circ O_2$ quenchers reduced the bactericidal activity of the thin film whereas the addition of the •OH and H_2O_2 quenchers did not cause a statistically significant change in the number of *E. coli* colonies recovered in comparison to the CuNP thin film without quenchers ($p > 0.05$, Mann–Whitney *U* test). This suggested that the bactericidal activity of the thin film is due to the formation of both $^1O_2$ and $^\circ O_2$.

Figure 8B demonstrates the activity of ROS quenchers on the thin film against *S. aureus*. $^1O_2$ was the only quencher that reduced the bactericidal activity of the thin film as the addition of the •OH, H_2O_2, and $^\circ O_2$ quenchers did not cause a statistically significant change in the number of *S. aureus* colonies recovered in comparison to the CuNP thin film without quenchers ($p > 0.05$, Mann–

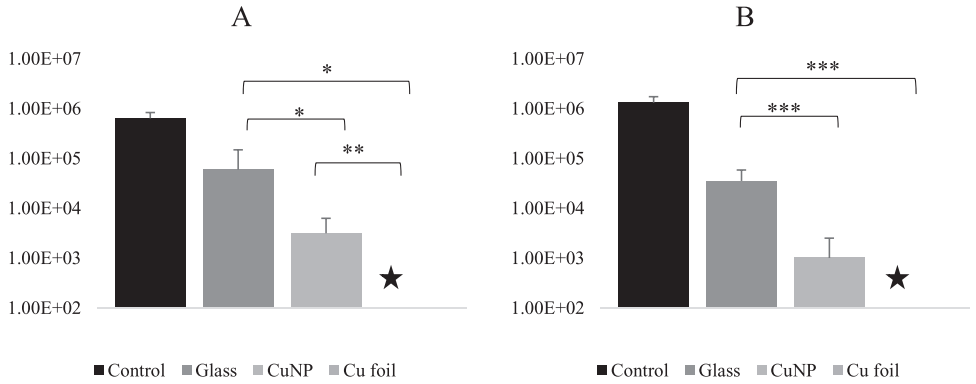

FIGURE 7 Antimicrobial activity of samples against (A) *E. coli* and (B) *S. aureus* after spraying 10^6 CFU mL^{-1}. The control was the control inoculum that had not been treated. The glass was the control glass that was included as the negative control and copper foil as the positive control. Star () indicates the copper foil for which the count was below the detection limit of 10^2 CFU mL^{-1}. * means $p \leq 0.05$, ** means $p \leq 0.01$, and *** means $p \leq 0.001$. Data presented as mean ± SD.

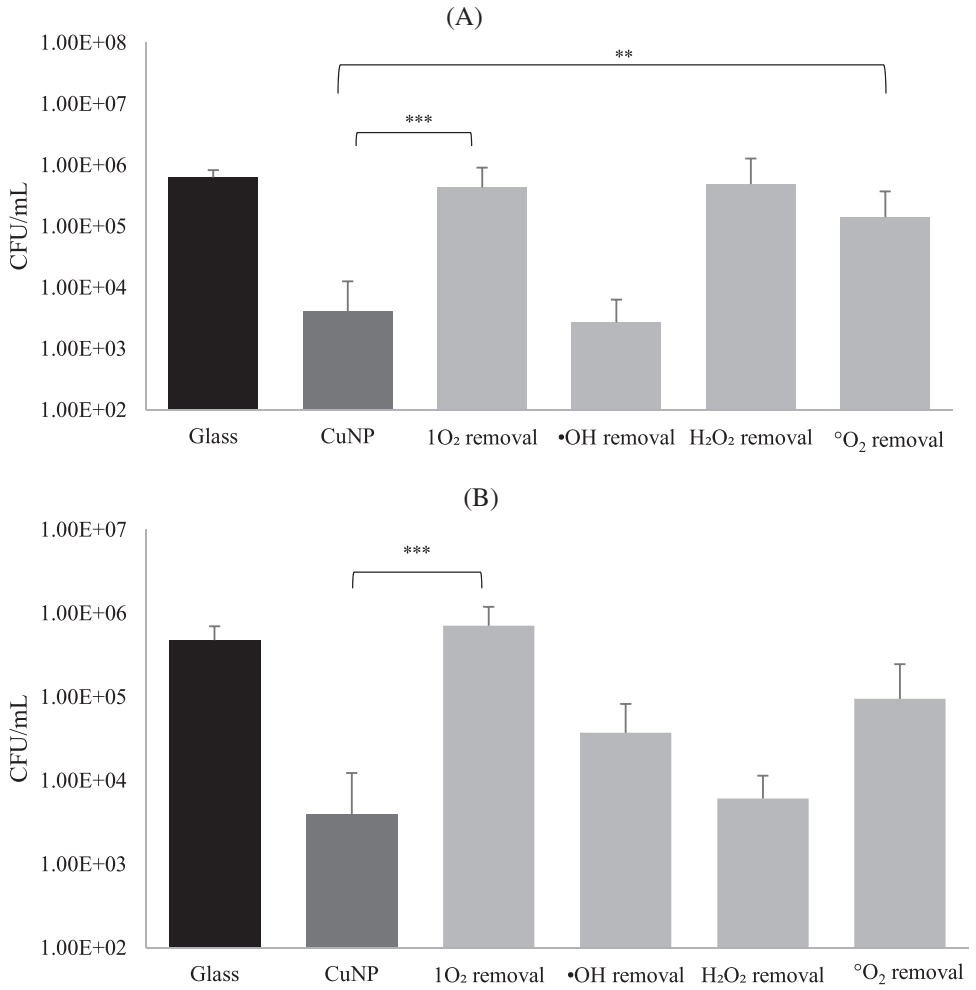

FIGURE 8 Bactericidal activity of the copper nanoparticle thin film (CuNP) after adding quenching agents that quench the different reactive oxygen species (ROS) with (A) *E. coli* and (B) *S. aureus*. The ROS were singlet oxygen ($^1O_2$), hydroxyl radicals (•OH), hydrogen peroxide (H_2O_2), and superoxide radicals ($^\circ O_2$). Control glass was included as the negative control and the CuNP film without quenchers as a positive control. ** means $p \leq 0.01$ and *** means $p \leq 0.001$. Data presented as mean ± SD.

Whitney *U* test). Thus, it was deduced that the formation of $^1O_2$ was responsible for the CuNP film's activity against *S. aureus*.

From this, we can deduce that the formation of $^1O_2$ is a crucial element of the CuNP film's activity against both bacterial species. While H_2O_2 was significant for the bactericidal activity of the CuNP film against *E. coli*, it did not have the same effect on *S. aureus*. It is understood that H_2O_2 and $^1O_2$ are less reactive than •OH and $^\circ O_2$, as the former can be detoxified by endogenous antioxidants, whereas the latter cannot.[57,58] Hence, if a thin film can demonstrate an ability to induce a response by •OH and $^\circ O_2$, it can ensure better antibacterial activity. The formation of $^1O_2$ from the CuNP thin film demonstrates a highly effective method of antibacterial performance that is resistant to endogenous antioxidants, as seen in Figure 8.

4 | DISCUSSION

To further study the impact of CuNPs on ROS generation, it is important to understand what causes the formation of excess ROS. Though the production of ROS through a Fenton-like and Haber–Weiss reaction is possible, the lack of an acidic environment in this study makes it an unfavorable pathway nonetheless, still possible.[59,60] The more likely cause of excess ROS formation in this study is that the CuNPs themselves may be responsible for the generation of ROS as small nanoparticles can infiltrate the bacterial cell membrane.[61–63] Such penetration has the potential to disrupt membrane integrity, leading to subsequent cellular damage and, eventually, cell lysis.[64–67] One study found CuNPs to penetrate bacteria, potentially interacting with phosphorus and sulfur-containing compounds like DNA due to their high affinity.[68] The precise mechanisms governing the entry of CuNPs into bacterial cells remain incompletely understood, with outcomes likely contingent upon specific conditions and the unique characteristics of the nanoparticles and bacteria involved.

Additionally, an alternative contributor to ROS generation is the formation of copper ions, that can enter the bacterial cell and induce excess ROS production.[26,68,69] Cu^+ and Cu^{2+}, derived from copper oxidation and leaching, may traverse bacterial cell membranes via active transport mechanisms facilitated by dedicated endogenous copper transporters. In one study, CuNP caused DNA degradation in *E. coli*, and the effect was primarily mediated by Cu^{2+} ions leached from the nanoparticles rather than ROS production.[69] Cu^{2+} ions could combine with the plasma membrane through electrostatic attraction, altering membrane permeability and leading to ion and metabolite leakage. Additionally, Cu^{2+} ions strongly interacted with intracellular amino acids and proteases, resulting in protein denaturation. It would be beneficial to conduct similar studies on the CuNP thin films in this study to elucidate the impact of Cu^{2+} ions on antimicrobial performance. Due to their small size and charge, copper ions may also permeate bacterial cells through passive diffusion across the cell membrane. Notably, a previous study suggested that this mechanism might not be the primary cause of initial antimicrobial activity in the presence of magnesium; however, further assessments with copper formulations are warranted for a comprehensive understanding.[70]

5 | CONCLUSION

A CuNP suspension in a silica matrix was synthesized to form a sol–gel and then dip-coated onto a glass substrate. The sol–gel method is economically viable, scalable, and can be controlled to produce a uniform, high-purity thin film. The CuNPs were successfully deposited into the films without oxidation, as determined by the Cu 2p peak on the XPS spectra, and the SEM images established a good distribution of the nanoparticles. The copper nanostructures in the SEM images and the hydrophobic contact angles created a surface that contributes to the thin film's ability to prevent biofilms from forming.

The CuNP thin films displayed antibacterial activity in humid conditions using the ISO protocol, achieving a 99.4% inactivation of *E. coli* and 99.2% of *S. aureus* after 1.5 hour incubation. This result is in accordance with the literature, as the effective inactivation of *E. coli* and *S. aureus* after a short incubation time is consistent with previous reports on the rapid bactericidal activity of CuNPs.[65,71–73] Additional tests with ROS quenchers revealed that singlet oxygen is the primary ROS responsible for the CuNP thin film's antibacterial activity. Nevertheless, the aerosolized inoculum resulted in a slight decline in the film's efficacy, indicating that the droplet method might be more appropriate for assessing the antimicrobial activity of thin films compared to the spray method. This observation implies that antimicrobial thin films may be better equipped to eliminate bacteria deposited by droplets rather than by sneezes and coughs.[74]

Overall, this study provides the basis for further research into developing advanced antimicrobial coatings, improving public health and preventing infectious disease transmission. Additional research is necessary to assess the coating's effectiveness against other bacterial species and its durability over time with regard to corrosion, ageing, and oxidation. Nevertheless, the potential of CuNP thin film remains high for a wide range of applications that require antibacterial coatings.

ACKNOWLEDGMENTS

The authors wish to thank S. Hurst from NSG Group for financial support and for useful discussion. The authors would also like to acknowledge the EPSRC Centre for Doctoral Training in Molecular Modelling and Material Science at University College London (EP/L015862/1) for financial support.

CONFLICTS OF INTEREST STATEMENT

There are no conflicts to declare.

DATA AVAILABILITY STATEMENT

Data are available on request from the authors.

ORCID

Intisar Salah https://orcid.org/0000-0002-4308-8191
Elaine Allan https://orcid.org/0000-0002-2703-7933
Sean P. Nair https://orcid.org/0000-0002-4658-9661
Ivan P. Parkin https://orcid.org/0000-0002-4072-6610

REFERENCES

1. N. H. L. Leung, *Nat. Rev. Microbiol.* **2021**, *19*, 528.
2. M. V. Bandres, P. Modi, S. Sharma, *Aspergillus Fumigatus*, StatsPearls Publishing, Treasure Island, Florida **2020**,.
3. S. S. Dunne, M. Ahonen, M. Modic, F. R. L. Crijns, M. M. Keinänen-Toivola, R. Meinke, C. W. Keevil, J. Gray, N. H. O'connell, C. P. Dunne, *J. Hosp. Infect.* **2018**, *99*, 250.
4. J. A. Belser, T. R. Maines, T. M. Tumpey, J. M. Katz, *Expert Rev. Mol. Med.* **2010**, *12*, e39.
5. P. Gastmeier, S. Stamm-Balderjahn, S. Hansen, F. Nitzschke-Tiemann, I. Zuschneid, K. Groneberg, H. Rüden, *Infect. Control Hosp. Epidemiol.* **2005**, *26*, 357.
6. S. A. Boone, C. P. Gerba, *Appl. Environ. Microbiol.* **2007**, *73*, 1687.
7. G. Brankston, L. Gitterman, Z. Hirji, C. Lemieux, M. Gardam, *Lancet Infect. Dis.* **2007**, *7*, 257.
8. M. Jayaweera, H. Perera, B. Gunawardana, J. Manatunge, *Environ. Res.* **2020**, *188*, 109819.
9. H. Li, F. Y. Leong, G. Xu, C. W. Kang, K. H. Lim, B. H. Tan, C. M. Loo, *Sci. Rep.* **2021**, *11*, 4617.
10. World Health Organization, Infection Prevention and Control of Epidemic- and PandemicProne Acute Respiratory Infections in Health Care, World Health Organization **2014**.
11. S. Ding, Z. W. Teo, M. P. Wan, B. F. Ng, *Build. Environ.* **2021**, *205*, 108239.
12. N. Van Doremalen, T. Bushmaker, D. H. Morris, M G. Holbrook, A. Gamble, B. N. Williamson, A. Tamin, J. L. Harcourt, N. J. Thornburg, S. I. Gerber, J. O. Lloyd-Smith, E. De Wit, V. J. Munster, *N. Engl. J. Med.* **2020**, *16*, 1564.
13. M. Birkett, L. Dover, C. Cherian Lukose, A. Wasy Zia, M M. Tambuwala, Á. Serrano-Aroca, *Int. J. Mol. Sci.* **2022**, *23*, 1162.
14. A. S. Karakoti, L. L. Hench, S. Seal, *Metals Mater. Soc.* **2006**, *58*, 77.
15. S. Shahzadi, N. Zafar, R. Sharif, *Intech. Open.* **2018**, *48*, 51.
16. A. Jilani, M. S. Abdel-Wahab, A. H. Hammad, *Advance Deposition Techniques for Thin Film and Coating* (Ed. N. N. Nikitenkov), Intech. Open, **2017**, p. 137.
17. I. A. Neacşu, A. I. Nicoară, O. R. Vasile, B. S. Vasile in *Nanobiomaterials in Hard Tissue Engineering* (Ed. A. M. Grumezescu), William Andrew Publishing **2016**, p. 271.
18. C. Glynn, D. Creedon, H. Geaney, E. Armstrong, T. Collins, M. A. Morris, C. O'Dwyer, *Sci. Rep.* **2015**, *5*, 11574.
19. K. Bondarczuk, Z. Piotrowska-Seget, *Cell Biol. Toxicol.* **2013**, *29*, 397.
20. H. Li, X. Zhou, Y. Huang, B. Liao, L. Cheng, B. Ren, *Front. Microbiol.* **2020**, *11*, 622534.
21. M. Y. Memar, R. Ghotaslou, M. Samiei, K. Adibkia, *Infect. Drug Resist.* **2018**, *11*, 567.
22. Y. Hong, J. Zeng, X. Wang, K. Drlica, X. Zhao, *Proc. Natl. Acad. Sci. USA* **2019**, *116*, 10064.
23. Y.-C. Wang, M. H. Engelhard, D. R. Baer, D. G. Castner, *Anal. Chem.* **2016**, *88*, 3917.
24. E. Korin, N. Froumin, S. Cohen, *ACS Biomater. Sci. Eng.* **2017**, *3*, 882.
25. J V. Prado, A. R. Vidal, T. C. Durán, *Rev. Med. Chil.* **2012**, *140*, 1325.
26. H. T. Michels, S. A. Wilks, J. O. Noyce, C. W. Keevil, Copper Alloys for Human Infectious Disease Control. In proceedings of the Materials Science and Technology Conference, Pittsburgh, **2005**.
27. S. L. Warnes, V. Caves, C. W. Keevil, *Environ. Microbiol.* **2012**, *14*, 1730.
28. M. C. Biesinger, *Surf. Interface Anal.* **2017**, *49*, 1325.
29. P. Kumari, P. Majewski, *J. Nanomaterials* **2013**, *2013*, 1.
30. Y. Li, B. P Zhang, C.-H. Zhao, J.-X. Zhao, *J. Mater. Res.* **2012**, *27*, 3141.
31. C. Tuchinda, S. Srivannaboon, H. W. Lim, *J. Am. Acad. Dermatol.* **2006**, *54*, 845.
32. H. Hu, *Highlights in Sci. Eng. Technol.* **2023**, *48*, 230.
33. A. Krasowska, K. Sigler, *Front. Cell. Infect. Microbiol.* **2014**, *4*, 112.
34. C. Adlhart, J. Verran, N. F. Azevedo, H. Olmez, M. M. Keinänen-Toivola, I. Gouveia, L. F. Melo, F. Crijns, *J. Hosp. Infect.* **2018**, *99*, 239.
35. U. Mahanta, M. Khandelwal, A. S. Deshpande, *J. Mater. Sci.* **2021**, *56*, 17915.
36. G. B Hwang, K. Page, A. Patir, S. P. Nair, E. Allan, I. P. Parkin, *ACS Nano* **2018**, *12*, 6050.
37. X. H. Wu, Y. K. Liew, C.-W. Mai, Y. Y. Then, *Int. J. Mol. Sci.* **2021**, *22*, 3341.
38. Y. Chan, X. H. Wu, B. W. Chieng, N. A. Ibrahim, Y. Y. Then *Nanomaterials (Basel)* **2021**, *11*, 1046.
39. M. Liravi, H. Pakzad, A. Moosavi, A. Nouri-Borujerdi, *Prog. Org. Coat.* **2020**, *140*, 105537.
40. I. P. Parkin, R. G. Palgrave, *J. Mater. Chem.* **2005**, *15*, 1689.
41. C. R. Crick, I. P. Parkin, *Chem.* **2010**, *16*, 3568.
42. H. Wang, K. Wang, H. Lu, I. P. Parkin, X. Zhang, *ACS Appl. Polym. Mater.* **2020**, *2*, 4856.
43. Y. Bi, Z. Wang, L. Lu, X. Niu, Y. Gu, L. Wang, *Prog. Org. Coat.* **2019**, *133*, 387.
44. Z. Wang, Z. Wang, *Polymer* **2015**, *74*, 216.
45. M. Potts, *Microbiol. Rev.* **1994**, *58*, 755.
46. A. Hedge, *J. Microb. Biochem. Technol.* **2015**, *7*, 210.
47. E. Laskowska, D. Kuczyńska-Wiśnik, *Curr. Genet.* **2020**, *66*, 313.
48. A. L. Casey, D. Adams, T. J. Karpanen, P. A. Lambert, B. D. Cookson, P. Nightingale, L. Miruszenko, R. Shillam, P. Christian, T. S. J. Elliott, *J. Hosp. Infect.* **2010**, *74*, 72.

49. C. E. Santo, E. W Lam, C. G. Elowsky, D. Quaranta, D. W. Domaille, C. J. Chang, G. Grass, *Appl. Environ. Microb.* **2011**, *77*, 794.
50. J. Inkinen, R. Mäkinen, M. M. Keinänen-Toivola, K. Nordström, M. Ahonen, *Lett. Appl. Microbiol.* **2017**, *64*, 19.
51. A. Różańska, A. Chmielarczyk, D. Romaniszyn, A. Sroka-Oleksiak, M. Bulanda, M. Walkowicz, P. Osuch, T. Knych, *Int. J. Environ. Res. Public Health* **2017**, *14*, 813.
52. E. C. Cole, C. E. Cook, *Am. J. Infect. Control* **1998**, *26*, 453.
53. R. Dhand, J. Li, *Am. J. Respir. Crit. Care Med.* **2020**, *202*, 651.
54. L. S. Chawla, B. Beers-Mulroy, G. F. Tidmarsh, *Crit. Care Clin.* **2019**, *35*, 357.
55. K. Giannousi, A. Pantazaki, C. Dendrinou-Samara, in *Nanostructures for Antimicrobial Therapy* (Eds: A. Ficai, A. M. Grumezescu), Elsevier **2017**, pp. 515–529.
56. M. Fasnacht, N. Polacek, *Front Mol. Biosci.* **2021**, *8*, 671037.
57. F. Vatansever, W. C. M. A. De Melo, P. Avci, D. Vecchio, M. Sadasivam, A. Gupta, R. Chandran, M. Karimi, N. A. Parizotto, R. Yin, G. P. Tegos, M. R. Hamblin, *FEMS Microbiol. Rev.* **2013**, *37*, 955.
58. D. J. Dwyer, M. A. Kohanski, J. J. Collins, *Curr. Opin. Microbiol.* **2009**, *12*, 482.
59. L. Zhou, W. Song, Z. Chen, G. Yin, *Environ. Sci. Technol.* **2013**, *47*, 3833.
60. A. Jawad, Z. Chen, G. Yin, *Chin. J. Catal.* **2016**, *37*, 810.
61. M. Ozdal, S. Gurkok, *ADMET DMPK* **2022**, *10*, 115.
62. K. L. Chen, G. D. Bothun, *Environ. Sci. Technol.* **2014**, *48*, 873.
63. N.-Y. Lee, W.-C. Ko, P.-R. Hsueh, *Front. Pharmacol.* **2019**, *10*, 1153.
64. D.-N. Phan, N. Dorjjugder, Y. Saito, M. Q. Khan, A. Ullah, X. Bie, G. Taguchi, I.-S. Kim, *Mater. Today Commun.* **2020**, *25*, 101377.
65. X. Ma, S. Zhou, X. Xu, Q. Du, *Front. Surg.* **2022**, *9*, 905892.
66. L. Wang, C. Hu, L. Shao, *Int. J. Nanomedicine* **2017**, *12*, 1227.
67. T. Kruk, M. Gołda-Cępa, K. Szczepanowicz, L. Szyk-Warszyńska, M. Brzychczy-Włoch, A. Kotarba, P. Warszyński, *Colloids Surf. B* **2019**, *181*, 112.
68. M. Raffi, S. Mehrwan, T. M. Bhatti, J. I. Akhter, A. Hameed, W. Yawar, M. M Ul Hasan, *Ann. Microbiol.* **2010**, *60*, 75.
69. A. K. Chatterjee, R. Chakraborty, T. Basu, *Nanotechnology* **2014**, *25*, 135101.
70. H. Feng, G. Wang, W. Jin, X. Zhang, Y. Huang, A. Gao, H. Wu, G. Wu, P. K. Chu, *ACS Appl. Mater. Interfaces* **2016**, *8*, 9662.
71. I. Salah, I. P. Parkin, E. Allan, *RSC Adv.* **2021**, *11*, 18179.
72. M. L. Ermini, V. Voliani, *ACS Nano* **2021**, *15*, 6008.
73. D. Longano, N. Ditaranto, L. Sabbatini, L. Torsi, N. Cioffi, *Nano-Antimicrobials* **2011**, 85.
74. A. J. Cunliffe, P. D. Askew, I. Stephan, G. Iredale, P. Cosemans, L. M. Simmons, J. Verran, J. Redfern, *Antibiotics (Basel)* **2021**, *10*, 1069.

How to cite this article: I. Salah, E. Allan, S. P. Nair, I. P. Parkin, *Nano Select* **2024**, 2300134. https://doi.org/10.1002/nano.202300134